ChemComm

COMMUNICATION

View Article Online
View Journal | View Issue

Cite this: *Chem. Commun.*, 2019, 55, 969

Received 30th November 2018,
Accepted 18th December 2018

DOI: 10.1039/c8cc09544b

rsc.li/chemcomm

Self-assembling nanoprobes that display two-dimensional fluorescent signals for identification of surfactants and bacteria†

Shuangshuang Long,[ab] Qinglong Qiao,[a] Fei Deng,[ac] Lu Miao,*[a] Juyoung Yoon*[c] and Zhaochao Xu*[a]

The imidazolium-pyrene self-assembling nanoprobes can rapidly discriminate four types of surfactants. The surfactants disassembled the probes to turn on significant fluorescence and transform between a pyrene monomer and an excimer, generating a two-dimensional analysis map. The probes were further used to identify different bacterial species.

Surfactants as surface active agents are heavily used in chemical industry and biomedical systems. The amphiphilic molecular properties lower the surface tension between two liquids or between a liquid and a solid. Depending on the ionic properties of the hydrophilic head, surfactants are classified into four types: anionic, cationic, zwitterionic, and nonionic surfactants.[1] All these types of surfactants play an essential role in our daily lives. They are widely used in detergents, pesticides, shampoos, cosmetics, or other consumer formulations. And the demand for these products is increasing year by year. The global surfactant market is expected to register a compound annual growth rate (CAGR) of 3.54% from 2018 to 2023. However, the widespread use of surfactants results in the discharge of surfactant-containing wastewater into our environment, which is inevitable. The unregulated disposal of surfactants into soil, water or sediment causes environmental pollution.[2–4] Surfactant toxicity has caused a worldwide alert leading to studies on environmental impacts of surfactants and the development of biodegradable ones. Accordingly, rapid and reliable detection methods for surfactant determination are required followed by effective treatments.

Conventional methods for surfactant identification include gas chromatography/mass spectrometry,[5] capillary electrophoresis,[6] and ion-selective electrodes.[7] But these methods suffered from some limitations, such as low reproducibility, unstable signal, tedious procedures, and the requirement of toxic solvents. Use of fluorescent probes for surfactant detection has emerged as an attractive method with easy operation and high sensitivity.[8–12] For example, Tang *et al.* developed an AIE fluorescent probe for the sensitive detection of anionic surfactants in neutral water.[13]

Furthermore, the 1,8-naphthalimide-derived polydiacetylene polymer showed the capability to respond to cationic surfactants with distinct color changes.[14] However, most of the reported probes can recognize only one single type of surfactant. Recently, a squaraine-based sensing array has been developed to discriminate three types of surfactants, anionic, cationic and nonionic.[15] However, more than three unspecific sensors should be reasonably designed and optimized. Recently, we reported a fluorescent probe complex **ZTRS-C18-Cd(II)** which first discriminated four types of surfactants.[16] However, the toxicity of the cadmium ion restricted its application. Thus, there's still a need for a probe that can discriminate all types of surfactants.

In this paper, we report environment-friendly fluorescent nanoprobes to discriminate all types of surfactants (Fig. 1). The imidazolium-derived pyrene compound **PI-1** aggregated to form nano-particles and the pyrene fluorescence was quenched by the aggregation effects.[17,18] Imidazolium acted as a binding site to recognize anions in the surfactants through electrostatic interaction. Pyrene is a classic fluorophore that emits unique fluorescence transformed between pyrene monomer and excimer emissions. Owing to this property, pyrene-based derivatives have been widely used to construct fluorescent probes, for example for the detection of ATP/ADP and heavy-metal ions.[19–23] After the addition of surfactants, the synergistic effects of electrostatic interaction and hydrophobic forces caused competitive binding between the surfactants and **PI-1**. This binding resulted in the disassembly of the nanoprobe to release the pyrene fluorophore and produce a fluorescence turn-on signal. Meanwhile, **PI-1** bound different types of surfactants and displayed varied pyrene-excimer and pyrene-monomer fluorescence, which produced different ratiometric signals. Subsequently, based on the

[a] *Key Laboratory of Separation Science for Analytical Chemistry, Dalian Institute of Chemical Physics, Chinese Academy of Sciences, Dalian 116023, China. E-mail: miaolu@dicp.ac.cn, zcxu@dicp.ac.cn*
[b] *University of Chinese Academy of Sciences, Beijing 100039, China*
[c] *Department of Chemistry and Nano Science, Ewha Womans University, Seoul 120-750, Korea. E-mail: jyoon@ewha.ac.kr; Fax: +82 2 3277 2384*

† Electronic supplementary information (ESI) available: Detailed experimental procedures, and additional tables and figures. See DOI: 10.1039/c8cc09544b

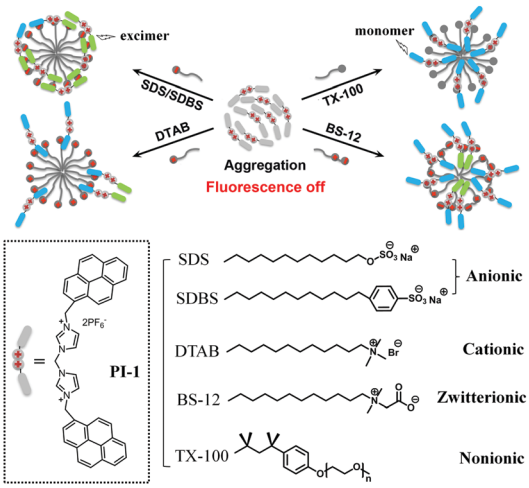

Fig. 1 The design of a self-assembling fluorescent nanoprobe to discriminate different types of surfactants.

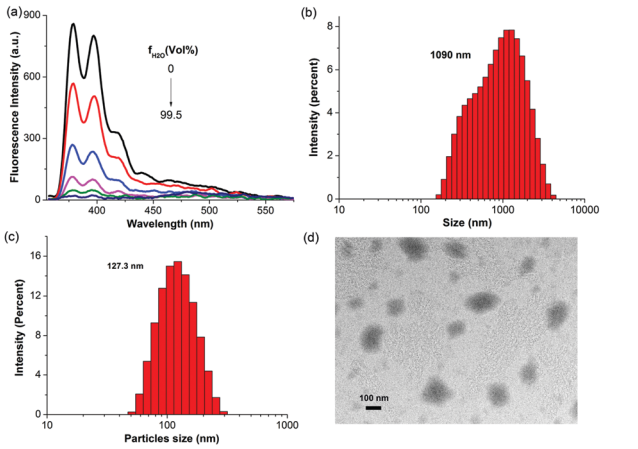

Fig. 2 (a) The fluorescence spectra of **PI-1** in DMSO/H_2O mixtures (λ_{ex} = 345 nm). (b) Dynamic light scattering (DLS) analysis of **PI-1** nanoaggregation. DLS (c) and TEM (d) analysis of **PI-1** in the presence of 400 μM SDS.

output signals of these two channels (fluorescence increase and ratiometric change), a two-dimensional analysis map could be established for visual interpretation of different types of surfactants. The nanoprobe can even distinguish different surfactants of the same type, such as SDS and SDBS, which are also anionic surfactants. The self-assembly nanoprobes were further used to identify different bacterial species whose cell walls were nearly negatively charged.

In the presence of co-solvents DMSO or CH_3CN, **PI-1** dissolved well in aqueous solution and could recognize G-Quadruplex DNA depending on the pyrene excimer/monomer ratiometric changes in our previous work.[24] And in aqueous solution with high water content, we found that **PI-1** aggregated to form nanoparticles. The aggregation property of **PI-1** was investigated by fluorescence detection in DMSO/H_2O mixtures. **PI-1** emitted strong pyrene-monomer fluorescence centered at 375 nm in DMSO solution, which indicated the dispersibility of the probe in polar solvents. When water was added to DMSO solutions, the fluorescence intensity decreased gradually. Up to 99.5% water content, the emission is hardly discerned (Fig. 2a). The dynamic light scattering (DLS) experiments confirm the formation of nanoparticles (Fig. 2b). The average diameter of the self-assembled nanoparticle was 1090 nm. The pyrene–pyrene stacking stabilized the self-assembling particles. The slight blue shift and obvious decrease in the absorption spectra also supported the formation of the aggregate (Fig. S1, ESI†).

The **PI-1** aggregate was then allowed to interact with four types of surfactants, including anionic surfactants sodium dodecyl sulfate (SDS) and sodium dodecyl benzene sulfonate (SDBS), cationic surfactant hexadecyl trimethyl ammonium bromide (DTAB), zwitterionic surfactant dodecyl dimethyl betaine (BS-12), and nonionic surfactant Triton X-100 (TX-100). First, the disassembling property of the probe was investigated by DLS analysis which provides direct evidence. The average diameter of the aggregate decreased from 1090 nm (Fig. 2b) to 127 nm (Fig. 2c) after the addition of 400 μM SDS (concentration lower than the critical micelle concentration). The transmission electron microscopy (TEM) image shows that the disassembled particles are irregular and the size is consistent with that determined by DLS analysis (Fig. 2d). Moreover, the slight red shift of the absorption spectra of **PI-1** after binding with surfactants demonstrated the disassembly of the aggregate (Fig. S2, ESI†).

To assess the fluorescence responses, the fluorescence spectra of the probe incubated with different concentrations of these surfactants were measured. As shown in Fig. 3, the titration experiments of the probe show varied fluorescence changes with the addition of different types of surfactants. For the anionic surfactants (SDS or SDBS), a small amount of surfactant can cause a significant pyrene-excimer fluorescence enhancement (centered at 482 nm) (Fig. 3a and b). With the addition of surfactants exceeding 1 mM, the fluorescence of pyrene-monomer began to appear and gradually increased. The addition of TX-100, on the contrary, only leads to the appearance and enhancement of pyrene-monomer fluorescence from the beginning to the end (centered at 375 nm) (Fig. 3c). For the zwitterionic surfactant BS-12 (Fig. 3d), pyrene-excimer emission appeared first and then pyrene-monomer emission was triggered with the addition of surfactants. The addition of cationic DTAB did not lead to any fluorescence changes up to a concentration higher than 10 mM with the appearance of weak monomer emission (Fig. 3e). Then these four types of surfactants can be well discriminated by the significantly different ratiometric signals (I_{375}/I_{482}) *versus* different concentrations (Fig. 3f). The differential fluorescence changes can even be directly observed by the naked eye with the assistance of a UV lamp (Fig. 3g). Both SDS and SDBS induced bright cyan fluorescence while the probe itself showed a faint cyan color. At the same time, the blueviolet color observed at different concentrations of TX-100 and BS-12 as well as at a high concentration of DTAB was well supported by the fluorescence spectra.

The ability of the nanoprobe to discriminate different types of surfactants can be explained by the different binding modes of the probe with the surfactants (Fig. 1), which should be due

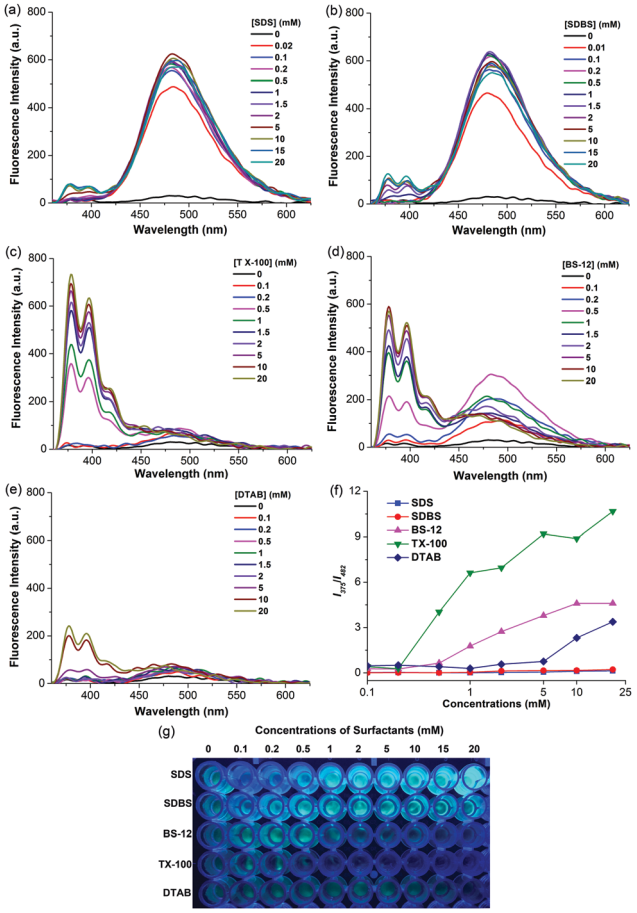

Fig. 3 The fluorescence spectra of **PI-1** (10 μM) treated with different concentrations (0–20 mM) of (a) SDS, (b) SDBS, (c) TX-100, (d) BS-12 and (e) DTAB. (f) Fluorescence ratiometric signal (I_{375}/I_{482}) of **PI-1** *versus* different concentrations of different surfactants. (g) Visible emission of **PI-1** titrated with different surfactants under UV irradiation. [**PI-1**] = 10 μM.

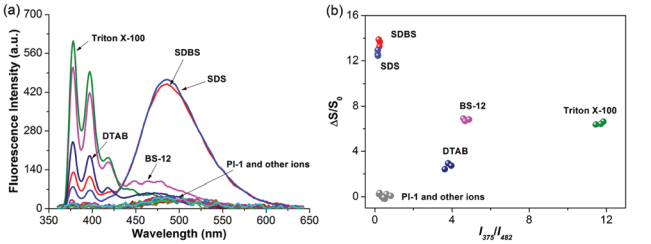

Fig. 4 (a) The fluorescence spectra of **PI-1** before and after incubating with SDS, SDBS, TX-100, BS-12, and DTAB, and other ions (ATP, GTP, CTP, PPi, SO_4^{2-}, PO_4^{3-}, HPO_4^{2-}, CO_3^{2-}, CH_3COO^-, Cl^-, Na^+, and K^+) in HEPES (20 mM, pH = 7.4), [**PI-1**] = 10 μM; [surfactants] = 20 mM; [ions] = 400 μM. (b) Two-dimensional plots obtained from a fluorescence response mode: the intensity increase ($\Delta S/S_0$) *vs.* fluorescence emission ratio (I_{375}/I_{482}).

to the difference in the charges of various types of surfactants and different environments formed by the hydrophilic head. The stronger electrostatic interaction between **PI-1** and SDS/SDBS disassembled the aggregate perfectly, and the hydrophilic environment caused by the electrostatic attraction caused the pair-stacking of the hydrophobic pyrene fluorophores. The nonionic surfactant TX-100 also disassembled the nanoprobe, and the hydrophobic environment was suitable for dissolution of pyrene and the separated pyrene molecules to exist as monomers. For zwitterionic BS-12, with the addition of many more surfactants, electrostatic repulsive force due to the positive charges of **PI-1** and BS-12 separated most of the pyrene molecules and hence gave rise to monomer emission. Due to the strong positive charge repulsion, it was reasonable to explain that DTAB cannot disassemble the aggregate.

Based on the fluorescence spectra of the probe with the addition of 20 mM of various surfactants, we can clearly identify these four types of surfactants, even including different surfactants of the same type, such as SDS and SDBS (Fig. 4a). The probe did not respond to common ions including Na^+, K^+, CO_3^{2-}, SO_4^{2-}, HPO_4^{2-}, CH_3COO^-, Cl^-, PO_4^{3-}, and PPi as well as adenosine phosphates (ATP, GTP, and CTP), which excluded the interference in complex environments during the test (Fig. 4a). Inspired by the method to reduce the dimensionality for visual interpretation used in fluorescent sensor arrays, a two-dimensional analysis map for visual interpretation of different types of surfactants, depending on the output signals of fluorescence increase ($\Delta S/S_0$) and ratiometric changes (I_{375}/I_{482}), could be established (Fig. 4b).

Since the nanoprobes showed high sensitivity towards various surfactants, especially for anionic SDS/SDBS, we were curious whether they were also sensitive to bacteria. The cell walls of all bacteria are nearly negatively charged,[25] although the surface structures of Gram-negative and Gram-positive bacteria are significantly different (Fig. 5a). In general, the Gram-negative bacterial surface is made up of two layers of plasma membrane. The outer membrane carries lipopolysaccharides (LPS) with negative charges. Gram-positive bacteria contain a single cell membrane surrounded by a thick layer of peptidoglycan, which is threaded through with abundant negatively charged teichuronic acids and lipoteichoic acids.

To verify the sensitivity of the probe, nine different species of bacterial suspensions (Table S1, ESI†) were separately added to the aqueous solution of the nanoprobes. As shown in Fig. 5b, the probe displayed turn-on fluorescence towards both Gram-negative and Gram-positive bacteria. Moreover, differential emission spectra including both pyrene excimer (centered at 482 nm) and monomer (centered at 375 nm) fluorescence have been obtained for different bacteria. The spectral profile is very similar to that of anionic SDS/SDBS (Fig. 4a). The bacteria may play a similar role to that of anionic SDS/SDBS, which is to disassemble the aggregate and form pyrene–pyrene stacking. A two-dimensional map with plots depending on changes in both fluorescence intensity ($\Delta S/S_0$) and emission ratios (I_{482}/I_{375}) is also established for identification of bacteria as shown in Fig. 5c. Although there was some overlap between *E. coli* and *C. freundii*, all the other bacteria were successfully discriminated by visual observation. Surprisingly, besides the species, the probe can also identify the Gram-positive and Gram-negative properties of the bacteria (Fig. 5c). From the fluorescence spectra (inset of Fig. 5b), we noted that Gram-negative bacteria have a stronger tendency to induce pyrene monomer emissions.

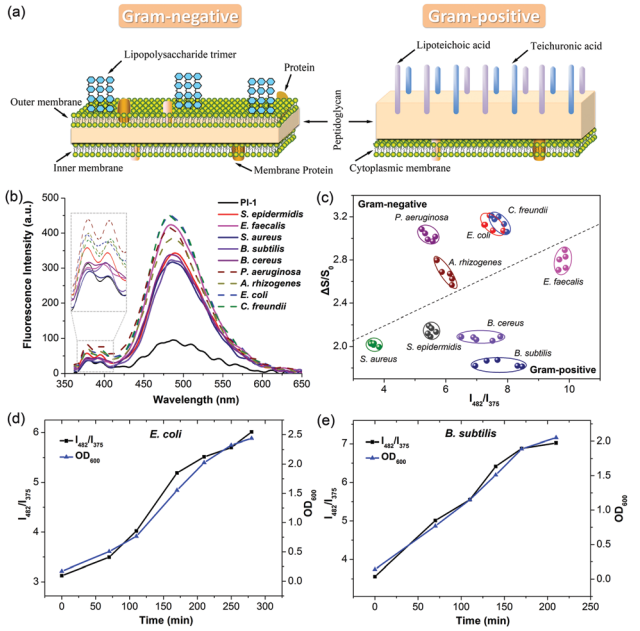

Fig. 5 Qualitative and quantitative analysis of **PI-1** for bacteria. (a) The schematic structure of Gram-negative and Gram-positive bacterial surfaces. (b) The fluorescence spectra of the probe (10 μM) treated with nine species of bacteria (OD_{600} = 0.5), respectively. (c) Two-dimensional plots of fluorescence increase ($\Delta S/S_0$) *versus* fluorescence emission ratio (I_{482}/I_{375}). Each circular region represents one single bacterial species, and each species has five replicates. Growth curves of (d) *E. coli* DH5α and (e) *B. subtilis* monitored by both OD_{600} and fluorescence emission ratio (I_{482}/I_{375}) of the probe.

This must be attributed to the significant difference in the cell walls of Gram-negative and Gram-positive bacteria. Like bacteria stained with crystal violet, Gram-positive bacteria may combine with imidazolium-derived pyrene more readily. Furthermore, the ratiometric properties endowed the probe with the ability to quantitatively detect bacteria. By employing both optical density (OD_{600}) and fluorescence emission ratio (I_{482}/I_{375}), we monitored the growth of *E. coli* and *B. subtilis* tested at the same time, that is for Gram-negative and Gram-positive bacteria, respectively (Fig. 5d, e and Fig. S3, ESI†). The growth curves obtained from these two methods showed a good overlap, which demonstrates the capability of the probe for quantitative analysis of bacteria (Fig. 5d and e). Therefore, the response of the probe towards various bacteria indicated that the probe can monitor the differences in the universal components of the bacterial surface. More importantly, the above results showed that the probe had high sensitivity and selectivity for identification of bacteria. In addition, the binding induced turn-on fluorescence enabled the bacteria test without a wash-out process.

In conclusion, we have developed a simple and rapid strategy for the identification of surfactants and bacteria by using a small molecule fluorescent probe **PI-1**. Through the synergistic effects of electrostatic and hydrophobic interaction, all four types of surfactants can be discriminated by both the concentration-dependent ratiometric signal (I_{375}/I_{482}) and the 2D map formed from the two channel signals, fluorescence increase and ratiometric signal. Furthermore, the high sensitivity and the signal amplification effect enabled the probe to generate unique emission fingerprints for diverse bacteria. Using this strategy, we can not only discriminate the different species of bacteria, but also determine the Gram-positive and Gram-negative properties of bacteria. Since nowadays bacterial infection is one of the major causes of human diseases and mortality in the world, rapid and efficient identification of bacteria is of great importance to help doctors administer targeted treatment. The strategy reported in this paper shows great potential for application in clinical diagnostics.

This work was financially supported by the National Natural Science Foundation of China (21878286, 21502189) and DICP (DMTO201603, TMSR201601). J. Y. acknowledges the support from the National Research Foundation of Korea (NRF) (No. 2012R1A3A2048814).

Conflicts of interest

There are no conflicts to declare.

Notes and references

1 M. J. Rosen and J. T. Kunjappu, *Surfactants and interfacial phenomena*, John Wiley & Sons, 2012.
2 W. H. Chan, A. W. M. Lee and J. Lu, *Anal. Chim. Acta*, 1998, **361**, 55.
3 J. Jensen, *Sci. Total Environ.*, 1999, **226**, 93.
4 M. G. Murphy, M. Al-Khalidi, J. F. S. Crocker, S. H. Lee, P. O'Regan and P. D. Acott, *Chemosphere*, 2005, **59**, 235.
5 L. Ripoll-Seguer, M. Beneito-Cambra, J. M. Herrero-Martinez, E. F. Simó-Alfonso and G. Ramis-Ramos, *J. Chromatogr. A*, 2013, **1320**, 66.
6 K. Heinig, C. Vogt and G. Werner, *Analyst*, 1998, **123**, 349.
7 J. Sánchez and M. del Valle, *Crit. Rev. Anal. Chem.*, 2005, **35**, 15.
8 X. Chen, S. Kang, M. J. Kim, J. Kim, Y. S. Kim, H. Kim, B. Chi, S. J. Kim, J. Y. Lee and J. Yoon, *Angew. Chem., Int. Ed.*, 2010, **49**, 1422.
9 E. Climent, C. Gimenez, M. D. Marcos, R. Martinez-Manez, F. Sancenon and J. Soto, *Chem. Commun.*, 2011, **47**, 6873.
10 Y. Chen, T. Zhang, X. Gao, W. Pan, N. Li and B. Tang, *Chin. Chem. Lett.*, 2017, **28**, 1983.
11 M. Pal, R. K. Singh and S. Pandey, *ChemPhysChem*, 2015, **16**, 2538.
12 Y. Li, C. Xu, C. Shu, X. Hou and P. Wu, *Chin. Chem. Lett.*, 2017, **28**, 1961.
13 M. Gao, L. C. Wang, J. J. Chen, S. W. Li, G. H. Lu, L. Wang, Y. J. Wang, L. Ren, A. J. Qin and B. Z. Tang, *Chem. – Eur. J.*, 2016, **22**, 5107.
14 D. E. Wang, L. Zhao, M. S. Yuan, S. W. Chen, T. Li and J. Wang, *ACS Appl. Mater. Interfaces*, 2016, **8**, 28231.
15 B. H. Li, W. W. Li, Y. Q. Xu, J. Li, J. Tu and S. G. Sun, *Chem. Commun.*, 2015, **51**, 14652.
16 F. Deng, S. Long, Q. Qiao and Z. Xu, *Chem. Commun.*, 2018, **54**, 6157.
17 J. R. Lakowicz, *Principles of Fluorescence Spectroscopy*, Plenum Press, New York, 1999.
18 I. Suzuki, M. Ui and A. Yamauchi, *J. Am. Chem. Soc.*, 2006, **128**, 4498.
19 Z. Xu, N. J. Singh, J. Lim, J. Pan, H. Kim, S. Park, K. S. Kim and J. Yoon, *J. Am. Chem. Soc.*, 2009, **131**, 15528.
20 Z. Xu, D. R. Spring and J. Yoon, *Chem. – Asian J.*, 2011, **6**, 2114.
21 S. Wang, L. Ding, J. Fan, Z. Wang and Y. Fang, *ACS Appl. Mater. Interfaces*, 2014, **6**, 16156.
22 Y. Wu, J. Wen, H. Li, S. Sun and Y. Xu, *Chin. Chem. Lett.*, 2017, **28**, 1916.
23 S. Leng, Q. Qiao, Y. Gao, L. Miao, W. Deng and Z. Xu, *Chin. Chem. Lett.*, 2017, **28**, 1911.
24 H. N. Kim, E. Lee, Z. Xu, H. Kim, H. Lee, J. Lee and J. Yoon, *Biomaterials*, 2012, **33**, 2282.
25 V. P. Harden and J. O. J. Harris, *Bacteriology*, 1953, **65**, 198.